

# Geophysical Research Letters

## RESEARCH LETTER

10.1029/2020GL090344

### Special Section:

The COVID-19 pandemic: linking health, society and environment

### Key Points:

- The global airborne NO<sub>2</sub> concentration steeply decreased over the vast majority of COVID-19-hit areas
- The total number of newly confirmed cases reached an inflection point about two weeks after the lockdown
- NO<sub>2</sub> satellite measurement can be adopted as an environmental lockdown indicator

### Correspondence to:

J. Huang,  
[hjp@lzu.edu.cn](mailto:hjp@lzu.edu.cn)

### Citation:

Lian, X., Huang, J., Zhang, L., Liu, C., Liu, X., & Wang, L. (2021). Environmental indicator for COVID-19 non-pharmaceutical interventions. *Geophysical Research Letters*, 48, e2020GL090344. <https://doi.org/10.1029/2020GL090344>

Received 25 AUG 2020

Accepted 14 DEC 2020

## Environmental Indicator for COVID-19 Non-Pharmaceutical Interventions

Xinbo Lian<sup>1</sup>, Jianping Huang<sup>1,2</sup> , Li Zhang<sup>1</sup> , Chuwei Liu<sup>1</sup>, Xiaoyue Liu<sup>1</sup> , and Lina Wang<sup>3</sup>

<sup>1</sup>Collaborative Innovation Center for Western Ecological Safety, College of Atmospheric Sciences, Lanzhou University, Lanzhou, China, <sup>2</sup>CAS Center for Excellence in Tibetan Plateau Earth Sciences, Beijing, China, <sup>3</sup>Gansu Province Environmental Monitoring Center, Lanzhou, China

**Abstract** A novel coronavirus (COVID-19) has caused viral pneumonia worldwide, posing a major threat to international health. Our study reports that city lockdown is an effective way to reduce the number of new cases and the nitrogen dioxide (NO<sub>2</sub>) concentration can be used as an environmental lockdown indicator to evaluate the effectiveness of lockdown measures. The airborne NO<sub>2</sub> concentration steeply decreased over the vast majority of COVID-19-hit areas since the lockdown. The total number of newly confirmed cases reached an inflection point about two weeks since the lockdown and could be reduced by about 50% within 30 days of the lockdown. The stricter lockdown will help newly confirmed cases to decline earlier and more rapidly, and at the same time, the reduction rate of NO<sub>2</sub> concentration will increase. Our research results show that NO<sub>2</sub> satellite observations can help decision makers effectively monitor and manage non-pharmaceutical interventions in the epidemic.

**Plain Language Summary** Since governments adopted epidemic control measures, NO<sub>2</sub> levels in most of the affected regions dropped significantly, and NO<sub>2</sub> satellite data can be used as an environmental indicator of lockdown and can help explain the implementation of government non-pharmaceutical interventions.

### 1. Introduction

Large-scale COVID-19 viral pneumonia through human-to-human transmission poses a severe and acute public health emergency (C. Huang et al., 2020; Li et al., 2020). As the epidemic worsened, most countries imposed city lockdown and quarantine measures to reduce transmission to control the epidemic. The Chinese government has gradually implemented a city-wide quarantine of Wuhan and several surrounding cities as of 23 January, flights and trains to and from Wuhan have been suspended, and public transport has been halted (Cyranoski et al., 2020; Wu et al., 2020). The entire northern Italy was quarantined since 9 March 2020, and three days later the government extended it to the whole country (Paterlini, 2020). The Spanish government declared a national emergency, starting on 15 March (Legido-Quigley et al., 2020). In Germany, since 18 March, 16 states have closed, public gatherings of more than two people have been banned, and most shops except supermarkets and pharmacies have closed (Dehning et al., 2020).

The worldwide lockdown, which was imposed to stop the spread of the novel coronavirus, not only caused an economic downturn but also appeared to result in cleaner air in urban areas usually heavily affected by pollution (Lian et al., 2020; Schiermeier, 2020). The most important measure of the lockdown policy was the reduction of traffic and control personnel flow, and traffic pollution is an important factor influencing air quality and public health. Vehicle exhaust and evaporation emissions are the main emission sources of ozone and secondary particle precursors near the ground in cities and regions (Zhou et al., 2019; Yuan et al., 2013), and the spatial variation of nitrogen dioxide (NO<sub>2</sub>), fine particulate matter (PM<sub>2.5</sub>), and black carbon (BC) may also be significant affected by traffic flow density (Clougherty et al., 2013). A study in Los Angeles showed that nitrogen oxides (NO<sub>x</sub>) were identified as a source of pollution for light vehicles, with NO<sub>2</sub>, NO<sub>x</sub>, carbon dioxide (CO<sub>2</sub>), BC, and fine particle number (PN<sub>fine</sub>) identified as diesel exhaust sources (Fan et al., 2018; Tessum et al., 2018). In South Korea, source analysis studies have shown that there is a high correlation between estimated traffic volume and NO<sub>2</sub> concentration (Kim et al., 2015). NO<sub>2</sub> levels can be used as a proxy for exposure to traffic-related composite air pollution and to assess the impact of scenarios designed to reduce traffic-related emissions (Brnnum-Hansen et al., 2018; Johansson et al., 2017).

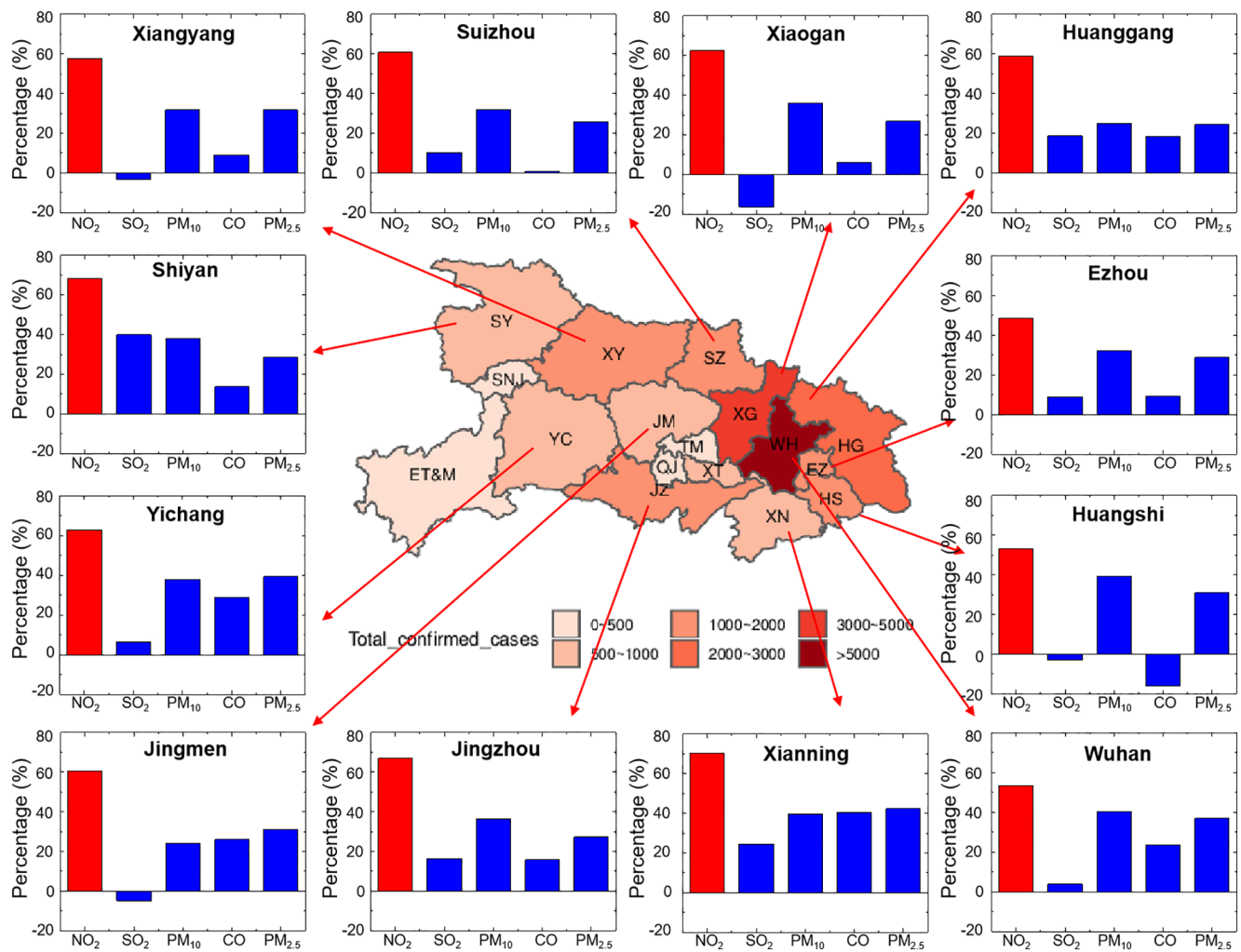


**Figure 1.** The improvement rate of the major pollutants and the distribution of the accumulated epidemic numbers in each city of Hubei Province one month since the lockdown.

In this report, we study the parameters of environmental indicators for city lockdown. Using the automatic ground detection data and satellite data to analyze the trend of lockdown and the total confirmed new cases in major cities in China, and using satellite data to further study the impact of lockdown on virus transmission in countries mainly severely affected by the epidemic, in order to help policymakers to formulate effective control measures to reduce the spread of COVID-19.

## 2. Data and Measurement

The ground observation data of five pollutants: PM<sub>2.5</sub>, particulate matter (PM<sub>10</sub>), sulfur dioxide (SO<sub>2</sub>), NO<sub>2</sub>, and carbon monoxide (CO) in cities in Hubei Province were selected for analysis, data source: <http://waqi.info/>. The data from 24 January 2020, to 23 February 2020, are selected as the representative data since the lockdown, and 24 December 2019, to 23 January 2020 as the before lockdown data (Figure 1). The automatic monitoring of PM<sub>2.5</sub> and PM<sub>10</sub> adopts the micro-oscillating balance method and the  $\beta$ -absorption method, respectively. SO<sub>2</sub> was determined by the ultraviolet fluorescence method, NO<sub>2</sub> by the chemiluminescence method, CO by the nondispersion infrared absorption method and gas filter correlation infrared absorption method. The average concentration of major cities with severe epidemic diseases was selected as the representative of NO<sub>2</sub> concentration of China, including Wuhan, Nanchang, Guangzhou, Hangzhou, Changsha, Beijing, Shanghai, Hefei, and Zhengzhou.

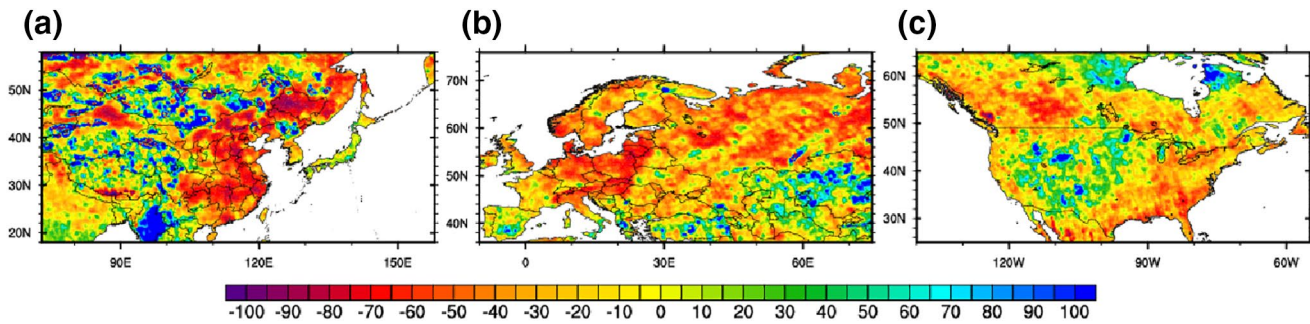


**Figure 2.** The relative variation in the monthly average tropospheric NO<sub>2</sub> concentration before and since the lockdown. (a) East Asia; (b) Western Europe; and (c) North America. Source: Analysis of data from the NASA Ozone Monitoring Instrument (OMI).

This paper adopted the level 3 daily global gridded ( $0.25 \times 0.25^\circ$ ) nitrogen dioxide product (OMNO2d) provided by the Ozone Monitoring Instrument (OMI) onboard the Aura satellite as the daily NO<sub>2</sub> data, which can be obtained from GES DISC ([https://cmr.earthdata.nasa.gov/search/concepts/C1266136111-GES\\_DISC.html](https://cmr.earthdata.nasa.gov/search/concepts/C1266136111-GES_DISC.html)). We selected the Column Amount NO<sub>2</sub> Trop product to calculate the changes in the tropospheric NO<sub>2</sub> concentration impacted by the control measures in East Asia, Western Europe and North America (Figure 2):

$$VA = \frac{N_2 - N_1}{N_1} \times 100\% \quad (1)$$

$$IR = \frac{N_1 - N_2}{N_1} \times 100\% \quad (2)$$

where VA is the relative variation ratio, IR is the improvement rate,  $N_1$  is the average concentration of the pollutant one month before the lockdown, and  $N_2$  is the average concentration of the pollutant one month since the lockdown.

The tropospheric NO<sub>2</sub> data from 1 January 2020 to 2 December 2020, were selected to analyze the variation in NO<sub>2</sub> over time in China. The NO<sub>2</sub> satellite data of Italy, Germany, France, the United States, Iran, and Switzerland is from the time of the first case in each country to 20 April 2020. Due to the satellite orbit, default values occur among the daily data that were determined via piecewise linear interpolation over time. Border data from the US Centers for Disease Control and Prevention (CDC) (<https://www.cdc.gov/epiinfo/support/downloads/shapefiles.html>) were selected to obtain the borders of each country. To remove the influence of weather factors, a 7-day moving average was calculated. To compare the relative changes among the different countries, the data for each country were standardized.

The daily number of confirmed cases in each country and region was obtained from the World Health Organization (WHO) (<https://www.who.int/>).

### 3. Results

#### 3.1. A Spatial Comparison of Pollutants Before and Since the Lockdown in Hubei Province

Figure 1 shows the change in pollutant concentration in Hubei Province one month before and since the lockdown of major cities. Compared with before the lockdown, NO<sub>2</sub>, SO<sub>2</sub>, PM<sub>10</sub>, CO, and PM<sub>2.5</sub> concentrations all decreased to a certain extent, while NO<sub>2</sub> experienced the most notable decrease. Since biomass and coal combustion are major SO<sub>2</sub> and CO sources, they exhibit the lowest rate of improvement (Q. Huang et al., 2012; Khalil et al., 1988). Both the PM<sub>2.5</sub> and PM<sub>10</sub> concentrations decreased to a certain extent (31.2% and 34.3%, respectively) as a result of the reduction in fugitive dust, particulate matter and important precursors produced by motor vehicles and factories (F. Huang et al., 2019). Studies have shown that the contribution of tail gas emissions to the total mass of PM<sub>2.5</sub> does not account for the main part, but mainly comes from other sources such as biomass combustion and the remote transmission of secondary particles (Chen et al., 2012). Therefore, the impact of strict traffic control during the lockdown on PM<sub>2.5</sub> is not notable, and the spatial difference is large, PM<sub>2.5</sub> is not suitable as a city lockdown indicator.

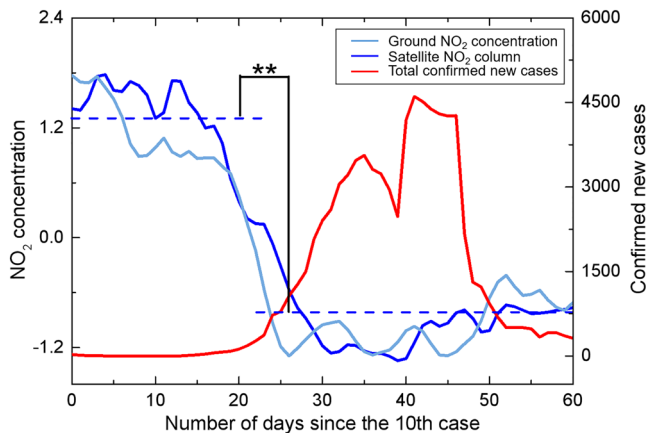


**Figure 3.** Temporal variation in the  $\text{NO}_2$  concentration and number of new cases in China. The dotted line indicates the average value of  $\text{NO}_2$  before and since the blockade. \*\* indicates significant difference at the 0.01 level (bilateral), and \* indicates significant difference at the 0.05 level (bilateral).

After the improvement of petroleum product quality standards, the  $\text{NO}_2$  emissions of per vehicle have decreased slightly, but the notable growth of vehicle ownership increased the proportion of  $\text{NO}_2$  traffic source emissions. In addition, after the implementation of emission standards for coal-fired power plants, multiple technical improvements greatly controlled the  $\text{NO}_2$  emissions from coal-fired sources, which also enhanced the correlation between  $\text{NO}_2$  and city lockdown effect (Liu et al., 2020). The effect of lockdown on  $\text{NO}_2$  was significantly greater than that on the other pollutants, with an average concentration reduction of approximately 60.3% (95% CI: 56.8%–64.0%) in Hubei, which can be applied as an environmental indicator of the lockdown effect.

### 3.2. Changes of Airborne $\text{NO}_2$ Plummet Over COVID-19-hit Area Since the Lockdown

In East Asia (Figure 2a), compared to before the lockdown, the total emissions of  $\text{NO}_2$  in eastern China have significantly decreased by approximately 56.6%. In South Korea, where the local government implemented the most extensive testing program and quarantined people infected with the virus without shutting down the entire city, monthly  $\text{NO}_2$  emissions were reduced by about 18.0% (Bauwens et al., 2020; Han, 2019). Recent studies have shown that in East Asia,  $\text{NO}_2$  experienced the most significant reductions by almost 83%, 33%, and 19% decrease in Wuhan, Seoul, and Tokyo, respectively compared with February 2019 (Ghahremanloo et al., 2020). In western Europe (Figure 2b), the monthly  $\text{NO}_2$  concentrations have decreased sharply in Italy by 47.5%, particularly in the north (82.4%), where the outbreak is the most severe. This could be due to the reduction in road traffic and the decrease in economic activities in the industrial heartland as a result of the widespread lockdown policy (Schiermeier, 2020). Other countries such as Germany, Denmark, and Poland also experienced notable reductions. This is consistent with the results of the European Environment Agency (EEA, 2020). In the case of Spain's two largest cities, in light of the sharp reduction in traffic, the reductions of  $\text{NO}_2$  concentrations were 62% and 50%, respectively, in Madrid and Barcelona (Baldasano, 2020). However, in certain areas, such as northern and southern Spain, the  $\text{NO}_2$  concentration has risen, possibly because of lax closure measures and increased emissions from coal-fired power plants, as well as meteorological factors (Curier et al., 2014). In the United States (Figure 2c), one month since the lockdown, the overall decline in  $\text{NO}_2$  is relatively small. The  $\text{NO}_2$  concentration is increasing significantly in the vast midwestern regions that have not yet been locked down.

### 3.3. The Temporal Evolution of the $\text{NO}_2$ Concentration and the Total Number of Newly Confirmed Cases in China

Since the strict city lockdown, the  $\text{NO}_2$  concentration in the main virus-affected cities in China decreased significantly (Figure 3). Consistent with the satellite data, the ground monitoring results showed that compared to the conditions before the lockdown, the monthly average  $\text{NO}_2$  concentration since the lockdown decreased approximately 55.7% (95% CI: 51.5%–59.6%) in eastern China. Since the lockdown, the total number of newly confirmed cases reaches an inflection point after approximately two weeks (the incubation period of the virus is 14 days). The most significant improvement was recorded in Hangzhou, where the  $\text{NO}_2$  concentration decreased approximately 68.1% and the epidemic was quickly brought under control in this region. Likewise, Zhengzhou, Changsha, Guangzhou, and Nanchang are good examples. Wuhan, the worst virus-affected area in China, also exhibited a downward trend. The total number of confirmed new cases reached 13,436 on February 12 due to the inclusion of clinically diagnosed cases (Wei et al., 2020), resulting in a new delayed peak in the figure.

The national emergency response has delayed the spread of the epidemic and greatly limited its range. Studies have shown that before emergency response initiation, the basic case reproduction number ( $R_0$ ) is 3.15, and after intervention measures were implemented in 95% of all places, the average  $R_0$  value has dropped

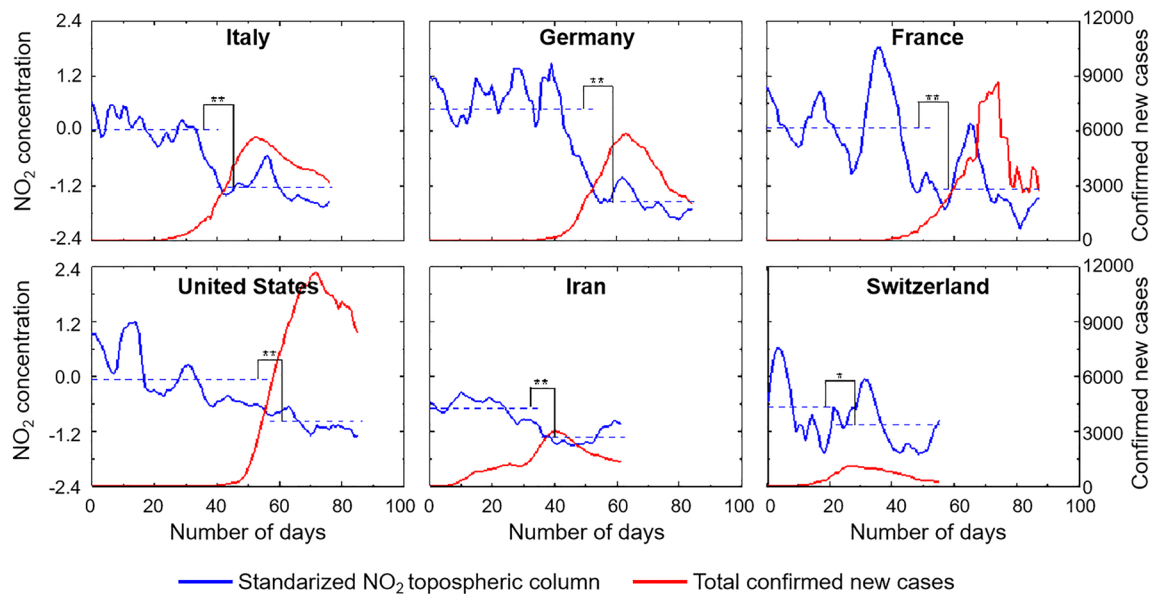


**Figure 4.** Temporal variation in the  $\text{NO}_2$  concentration and number of new cases in the COVID-19-hit areas. The dotted line indicates the average value of  $\text{NO}_2$  before and since the blockade. The starting time is when the first case was detected in the area. \*\* indicates significant difference at the 0.01 level (bilateral), and \* indicates significant difference at the 0.05 level (bilateral).

to 0.04, the total number of actual cases has decreased 96% (Tian et al., 2020). The decline in the case rate is related to the implementation of measures such as the suspension of public transportation in the city, the closure of entertainment venues and the ban on public gatherings. The content of  $\text{NO}_2$  can reflect the implementation intensity of these control policies.

#### 3.4. The Temporal Evolution of the $\text{NO}_2$ Concentration and the Total Number of Newly Confirmed Cases in the COVID-19-hit Areas Globally

About two weeks since the implementation of strict lockdown measures in COVID-19-hit area, the total number of newly confirmed cases in most regions has dropped, and  $\text{NO}_2$  emissions also decreased significantly (Figure 4). As a result, the strict lockdown of COVID-19-hit areas other than those in China is also effective and easy to implement. The lockdown measures might have already prevented tens of thousands of deaths in Europe (Flaxman et al., 2020). The occurrence time of the inflection point of the newly confirmed cases is mainly related to the implementation effect of non-pharmaceutical intervention measures, and the reduction rate of  $\text{NO}_2$  is also related to the policy implementation status. Therefore, the reduction rate of  $\text{NO}_2$  can be used to characterize the degree of non-pharmaceutical intervention to determine when the inflection point of newly confirmed cases appears. The  $\text{NO}_2$  emissions significantly decreased by an average of 36.6% and the total confirmed new cases reached an inflection point 12 days later since the lockdown in Italy. Studies have shown that 38,000 deaths have been averted in this country due to the implemented intervention measures (Flaxman et al., 2020).  $\text{NO}_2$  declined less (27.1%) in France, and the time for the total number of confirmed new cases to reach an inflection point was delayed. In Germany, the  $\text{NO}_2$  emissions decreased the most, by 54.7%, and the total number of confirmed new cases reached an inflection point within 8 days since the lockdown, which occurred earlier than in other countries. Due to the relatively low number of confirmed cases in Iran and Switzerland, with the decline of  $\text{NO}_2$  after the strict control, confirmed new cases also reached the inflection point earlier. In the the worst-affected states, United States,  $\text{NO}_2$  emissions decreased by an average of 43.1% in New York, Washington and California, and the total confirmed new cases dropped significantly, showing signs of easing.

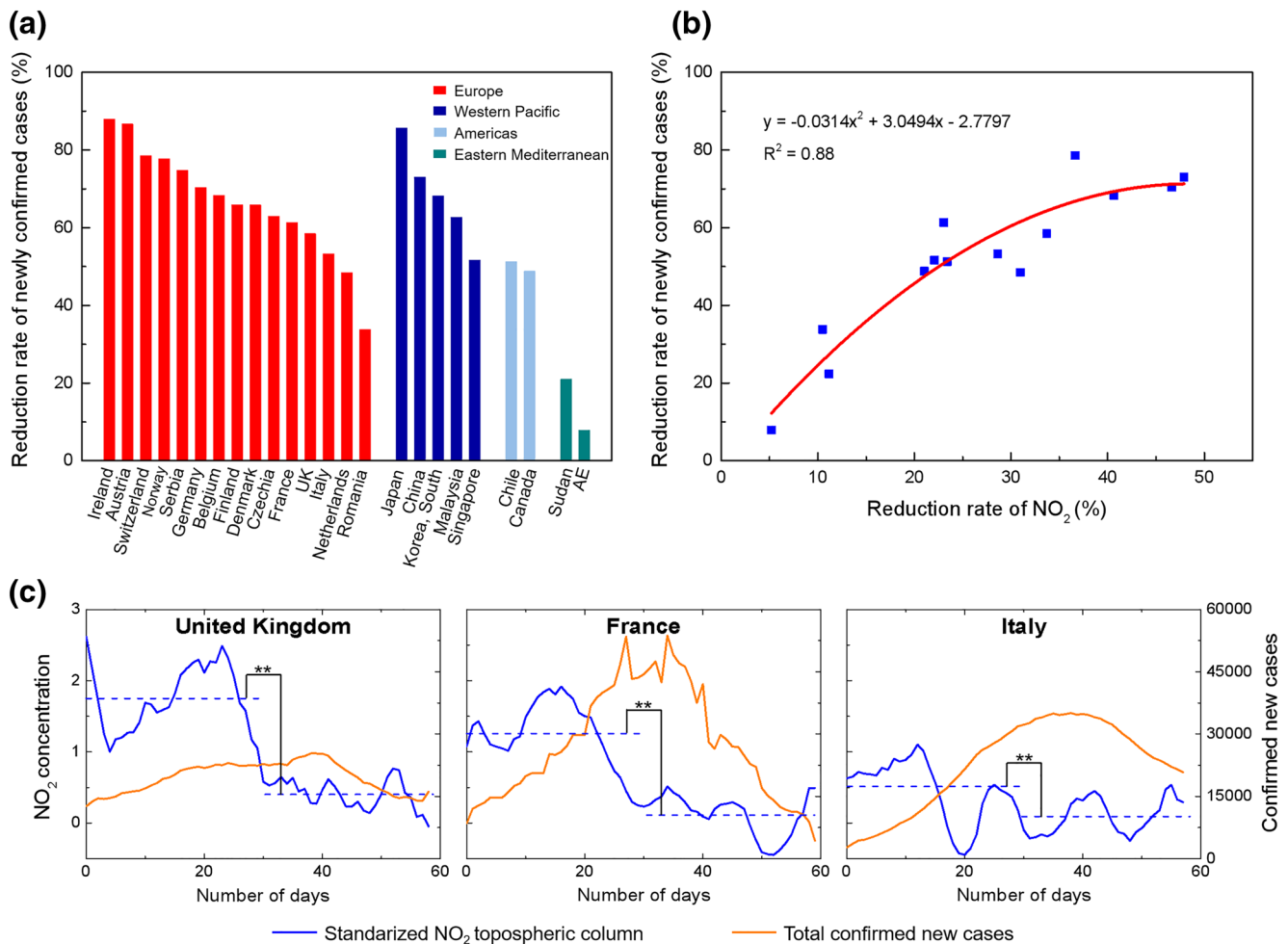


**Figure 5.** The results of the strict epidemic control measures. (a) The reduction rate of new confirmed cases within 30 days at the NO<sub>2</sub> mutation point; (b) Changes in the rate of decline in NO<sub>2</sub> and the reduction rate of newly confirmed cases since the implementation of strict epidemic control measures. (c) Temporal variation in the NO<sub>2</sub> concentration and number of new cases during the second wave of epidemics. The dotted line indicates the average value of NO<sub>2</sub> before and since the blockade. \*\* indicates significant difference at the 0.01 level (bilateral), and \* indicates significant difference at the 0.05 level (bilateral).

### 3.5. The Results Since the Epidemic Control in the COVID-19-hit Areas Globally

Following the implementation of strict epidemic control measures, the newly confirmed cases dropped by more than 50% within 30 days at the NO<sub>2</sub> mutation point, especially in most countries in Europe and the Western Pacific Region, where the decline was more significant (Figure 5a). The reduction in the number of newly confirmed cases is closely related to the intensity of interventions. The indicator effect of the reduction rate of NO<sub>2</sub> confirms that among the top 50 countries with the cumulative number of confirmed cases, stricter intervention is more conducive to epidemic control. When the NO<sub>2</sub> reduction rate is only about 25%, the intensity of the government intervention measures indicated will not have a significant effect on the control of the epidemic (Figure 5b). Studies have shown that only after the government authorities imposed a contact ban did the spreading rate ( $\lambda$ ) dropped to 0.09, which is lower than the recovery speed, and the exponential growth of new cases turned to decline (Dehning et al., 2020). In Wuhan, China, due to the strict lockdown, the estimated effective reproduction number  $R_t$  fell below 1.0 on 6 February 2020 (NO<sub>2</sub> mutation time) (Pan et al., 2020).

In addition, in the new wave of the outbreak in Europe, France, the United Kingdom, and other European countries are bringing back a lockdown and escalating restrictions. Consistent with the first wave of outbreaks, local NO<sub>2</sub> levels declined significantly with the implementation of non-pharmaceutical

LIAN ET AL.

interventions, and the number of newly confirmed cases declined within 14 days (Figure 5c). Therefore, it is feasible to use NO<sub>2</sub> as an environmental indicator for quantitative research, which helps to assess the efficacy and timing of non-pharmaceutical interventions to guide current and future responses to global pandemics.

#### 4. Conclusion and Discussion

Urbanization and rapid transportation system development accelerate the spread of COVID-19, and only strict containment measures can effectively prevent a second and third outbreak (Z. Huang et al, 2020; J. Huang et al., 2020). Studies have shown that it is difficult to reduce the number of cases significantly in a gradual multi-stage policy, and that such a policy decision implies that the government is willing to risk an increase in COVID-19 cases and deaths in exchange for decreased economic and isolation impacts, which may not be desirable from an objective point of view (Karnon, 2020). Our results show that approximately 15 days since the implementation of the lockdown policy, the number of newly confirmed cases will decline, and an earlier decline can occur with stricter lockdown measures. Although the immediate adoption of a lockdown policy may lead to many people being adversely affected financially, the impact is short-term, and the control of the epidemic is long-term. International guidance supports a range of mandatory social isolation measures, extensive case detection, and isolation and contact tracing. Compliance with quarantine directives is absolutely critical to saving lives, protecting the most vulnerable in society, and ensuring that the national security system can cope and care for the sick (Iacobucci, 2020).

NO<sub>2</sub> can be used as an environmental indicator to quantify the effectiveness and intensity of interventions and can be incorporated into assessments of the implementation of existing outbreak control measures in countries and into prediction of future scenarios and case numbers. In addition, NO<sub>2</sub> would help provide policymakers with information on strengthening, easing and selecting appropriate measures to contain COVID-19 and other future global pandemics. For details, please refer to the Global Prediction System of the COVID-19 Pandemic (<http://covid-19.lzu.edu.cn>). However, there are some areas where NO<sub>2</sub> concentrations are not influenced by local emissions. For example, the unexpected increase of NO<sub>2</sub> observed in other areas such as southern and northern Spain and parts of the United States could be due to the meteorological influences. Therefore, we need to find NO<sub>2</sub> mutation points to screen out areas suitable for this research method. Like Figure 5, if NO<sub>2</sub> drops significantly and there is a mutation point, then the number of newly confirmed cases in the region will also decrease. We selected the top 50 countries with cumulative confirmed cases and find the NO<sub>2</sub> mutation points in each affected area. The results showed that at the point of NO<sub>2</sub> mutation, in more than 70% of areas, newly confirmed cases dropped by more than 50%. In more than 23% of the regions, newly confirmed cases have dropped by more than 70%, such as Ireland, Austria, Germany, Japan, China, etc.

#### Conflict of Interest

The authors declare no conflicts of interest relevant to this study.

#### Data Availability Statement

The data sources for supporting this analysis are publicly available. We acknowledge the use of data products from the NASA Aura satellite missions ([https://cmr.earthdata.nasa.gov/search/concepts/C1266136111-GES\\_DISC.html](https://cmr.earthdata.nasa.gov/search/concepts/C1266136111-GES_DISC.html)). The daily confirmed cases of COVID-19 data are available from the World Health Organization (WHO) (<https://www.who.int/>). The air quality monitoring data in China are available from the World Air Quality Index project (<http://waqi.info/>). The border data are available from the US Centers for Disease Control and Prevention (<https://www.cdc.gov/epiinfo/support/downloads/shapefiles.html>). Graphics Software: All maps and plots were produced using licensed.

#### References

- Baldasano, J. M. (2020). COVID-19 lockdown effects on air quality by NO<sub>2</sub> in the cities of Barcelona and Madrid (Spain). *Science of the Total Environment*, 741, 140353.

#### Acknowledgments

The authors acknowledge the National Science Foundation of China (41521004) and the Gansu Provincial Special Fund Project for Guiding Scientific and Technological Innovation and Development (grant no. 2019ZX-06).

- Bauwens, M., Compennolle, S., Stavrou, T., Müller, J. F., Van Gent, J., Eskes, H., et al. (2020). Impact of coronavirus outbreak on NO<sub>2</sub> pollution assessed using TROPOMI and OMI observations. *Geophysical Research Letters*, *47*, e2020GL087978. <https://doi.org/10.1029/2020GL087978>
- Brnum-Hansen, H., Bender, A. M., Andersen, Z. J., Sørensen, J., Bønløkke, J. H., Boshuizen, H., et al. (2018). Assessment of impact of traffic-related air pollution on morbidity and mortality in Copenhagen Municipality and the health gain of reduced exposure. *Environment International*, *121*, 973–980.
- Chen, Y., Liu, Q., Geng, F., Zhang, H., Cai, C., Xu, T., et al. (2012). Vertical distribution of optical and micro-physical properties of ambient aerosols during dry haze periods in Shanghai. *Atmospheric Environment*, *50*, 50–59.
- Clougherty, J. E., Kheirbek, I., Eisl, H. M., Ross, Z., Pezeshki, G., Gorczynski, J. E., et al. (2013). Intra-urban spatial variability in winter-time street-level concentrations of multiple combustion-related air pollutants: The New York City Community Air Survey (NYCCAS). *Journal of Exposure Science & Environmental Epidemiology*, *23*, 232–240.
- Curier, R. L., Kranenburg, R., Segers, A. J. S., Timmermans, R. M. A., & Schaap, M. (2014). Synergistic use of OMI NO<sub>2</sub> tropospheric columns and LOTOS-EUROS to evaluate the NO<sub>x</sub> emission trends across Europe. *Remote Sensing of Environment*, *149*, 58–69.
- Cyranoski, D., & Silver, A. (2020). Wuhan scientists: What it's like to be on lockdown. *Nature News*, 24 JAN. <https://doi.org/10.1038/d41586-020-00191-5>
- Dehning, J., Zierenberg, J., Spitzner, F. P., Wibral, M., Neto, J. P., Wilczek, M., & Priesemann, V. (2020). Inferring change points in the spread of COVID-19 reveals the effectiveness of interventions. *Science*, *369*(6500), eabb9789.
- Fan, X., Dawson, J., Chen, M., Qiu, C., & Khalizov, A. (2018). Thermal stability of particle-phase monoethanolamine salts. *Environmental Science & Technology*, *52*, 2409–2417.
- Flaxman, S., Mishra, S., Gandy, A., Unwin, H. J. T., Mellan, T. A., Coupland, H., et al. (2020). Estimating the effects of non-pharmaceutical interventions on COVID-19 in Europe. *Nature*, *584*(7820), 257–261. <https://doi.org/10.1038/s41586-020-2405-7>
- Ghahremanloo, M., Lops, Y., Choi, Y., & Mousavinezhad, S. (2020). Impact of the COVID-19 outbreak on air pollution levels in East Asia. *Science of the Total Environment*, *754*, 142226.
- Han, K. M. (2019). Temporal analysis of OMI-observed tropospheric NO<sub>2</sub> columns over East Asia during 2006–2015. *Atmos*, *10*, 658.
- Huang, Q., Cheng, S., & Perozzi, R. E. (2012). Use of a MM5-CAMx-PSAT modeling system to study SO<sub>2</sub> source apportionment in the Beijing Metropolitan Region. *Environmental Modeling & Assessment*, *17*, 527–538.
- Huang, Z., Huang, J., Gu, Q., Du, P., Liang, H., & Dong, Q. (2020). Optimal temperature zone for the dispersal of COVID-19. *Science of the Total Environment*, *736*, 139487.
- Huang, J., Zhang, L., Liu, X., Wei, Y., Liu, C., Lian, X., et al. (2020). Global prediction system for COVID-19 pandemic. *Science Bulletin*, *65*(22), 1884–1887. <https://doi.org/10.1016/j.scib.2020.08.002>
- Huang, C., Wang, Y., Li, X., Ren, L., Zhao, J., Hu, Y., et al. (2020). Clinical features of patients infected with 2019 novel coronavirus in Wuhan, China. *The Lancet*, *395*(10223), 497–506. [https://doi.org/10.1016/s0140-6736\(20\)30183-5](https://doi.org/10.1016/s0140-6736(20)30183-5)
- Huang, F., Zhou, J., Chen, N., Li, Y., & Wu, S. (2019). Chemical characteristics and source apportionment of PM<sub>2.5</sub> in Wuhan, China. *Journal of Atmospheric Chemistry*, *76*, 245–262.
- Iacobucci, G. (2020). Covid-19: UK lockdown is “crucial” to saving lives, say doctors and scientists. *BMJ*, *368*, m1204. <https://doi.org/10.1136/bmj.m1204>
- Johansson, C., Lovenheim, B., Schantz, P., Wahlgren, L., Almstrom, P., Markstedt, A., et al. (2017). Impacts on air pollution and health by changing commuting from car to bicycle. *Science of the Total Environment*, *584*, 55–63.
- Karnon, J. (2020). A simple decision analysis of a mandatory lockdown response to the COVID-19 pandemic. *Applied Health Economics and Health Policy*, *18*, 329–331.
- Khalil, M. A. K., & Rasmussen, R. A. (1988). Carbon monoxide in an urban environment: Application of a receptor model for source apportionment. *JAPCA*, *38*, 901–906.
- Kim, Y., & Guldmann, J. M. (2015). Land-use regression panel models of NO<sub>2</sub> concentrations in Seoul, Korea. *Atmospheric Environment*, *107*, 364–373.
- Legido-Quigley, H., Mateos-Garcia, J. T., Campos, V. R., Gea-Sanchez, M., Muntaner, C., & McKee, M. (2020). The resilience of the Spanish health system against the COVID-19 pandemic. *The Lancet Public Health*, *5*, e251–e252.
- Lian, X., Huang, J., Huang, R., Liu, C., Wang, L., & Zhang, T. (2020). Impact of city lockdown on the air quality of COVID-19-hit of Wuhan city. *Science of the Total Environment*, *742*, 140556.
- Li, Q., Guan, X., Wu, P., Wang, X., Zhou, L., Tong, Y., et al. (2020). Early transmission dynamics in Wuhan, China, of novel coronavirus-infected pneumonia. *The New England Journal of Medicine*, *382*, 1199–1207.
- Liu, D., Deng, Q., Ren, Z., Zhou, Z., Song, Z., Huang, J., & Hu, R. (2020). Variation trends and principal component analysis of nitrogen oxide emissions from motor vehicles in Wuhan City from 2012 to 2017. *Science of the Total Environment*, *704*, 134987.
- Pan, A., Liu, L., Wang, C., Guo, H., Hao, X., Wang, Q., et al. (2020). Association of public health interventions with the epidemiology of the COVID-19 outbreak in Wuhan, China. *JAMA*, *323*, 1915–1923.
- Paterlini, M. (2020). Lockdown in Italy: personal stories of doing science during the COVID-19 quarantine. *Nature*.
- Schiermeier, Q. (2020). Why pollution is plummeting in some cities - but not others. *Nature*, *580*, 313.
- Tessum, M. W., Larson, T., Gould, T. R., Simpson, C. D., Yost, M. G., & Vedal, S. (2018). Mobile and fixed-site measurements to identify spatial distributions of traffic-related pollution sources in Los Angeles. *Environmental Science & Technology*, *52*, 2844–2853.
- The European Environment Agency (EEA). (2020). Air pollution goes down as Europe takes hard measures to combat coronavirus. *EEA News*, 25 Mar.
- Tian, H., Liu, Y., Li, Y., Wu, C., Chen, B., Kraemer, M. U. G., et al. (2020). An investigation of transmission control measures during the first 50 days of the COVID-19 epidemic in China. *Science*, *368*, 638–642.
- Wei, Y., Wei, L., Jiang, Y., Shen, S., Zhao, Y., Hao, Y., et al. (2020). Implementation of clinical diagnostic criteria and universal symptom survey contributed to lower magnitude and faster resolution of the COVID-19 epidemic in Wuhan. *Engineering*, *6*:1141–1146.
- Wu, J. T., Leung, K., & Leung, G. M. (2020). Nowcasting and forecasting the potential domestic and international spread of the 2019-nCoV outbreak originating in Wuhan, China: A modeling study. *Obstetrical and Gynecological Survey*, *75*(7), 399–400.
- Yuan, B., Hu, W., Shao, M., Wang, M., Chen, W., Lu, S., et al. (2013). VOC emissions, evolutions and contributions to SOA formation at a receptor site in eastern China. *Atmospheric Chemistry and Physics*, *13*, 8815–8832.
- Zhou, Z., Tan, Q., Liu, H., Deng, Y., Wu, K., Liu, C., & Zhou, X. (2019). Emission characteristics and high-resolution spatial and temporal distribution of pollutants from motor vehicles in Chengdu, China. *Atmospheric Pollution Research*, *10*, 749–775.

LIAN ET AL.